BME 590L: Machine Learning in Imaging Final Project: Optimization of the optics lens in the classification of Colorectal Cancer Histology

Po-Kang, Liu
Department of Biomedical Engineering
Duke University
Durham, NC 27705
pokang.liu@duke.edu

Abstract

Due to the progress of Artificial Intelligence (AI) and computer vision, using AI to conduct Computer-Aided Diagnosis (CAD) on the medical images such as histopathology has become a new research focus. However, a normal microscope is hard to extract the transparent optical characteristics and features in the common medical samples. In this study, I aim to add the optic mask in the microscope and optimize it to boost the CNN classification performance of Colorectal Cancer Histology. I simulate four different optics masks and two CNN architectures. The result shows that the unconstraint phase mask cascading with the Alexnet CNN have the highest performance compared with other architectures. While the RGB color filter would be the most practicable, cost-effective physical layer setup (66% accuracy).The segmentation task on the larger Colorectal Histology validates the feasibility of this framework. Our findings could aid the researchers to select the ideal optic mask, jointly optimizing with CNN, in developing more robust Computer Aid Diagnoses tools.

1 Introduction

1.1 Background and Challenges

Histopathology is the microscopic examination of diseased tissue. It is important in the diagnosis and treatment of cancer. [1]. Due to the progression of Artificial Intelligence (AI) technology, Computer-Aided Diagnosis (CAD) based on histopathological imaging has progressed rapidly in recent years [2]. The computer could perform a variety of histology image analysis tasks by Deep Learning architecture including detection and counting, segmentation, tissue classification, even grading and prognosis prediction [3].

Even though Deep Learning is a really robust method to analyze the biological images, a lot of medical samples have transparent optical characteristics and contain features that are hard to extract when acquiring images with a normal microscope [4]. Hence, the performance of Computer-Aided Diagnosis would be bounded.

1.2 Relative Works and Motivations

Recently, a novel idea has emerged to surpass the current limitation of CNN in medical diagnosis. Several studies attempted to jointly optimize the physical parameters of microscopy with CNN. A. Muthumbi and A. Chaware et al. optimized the microscope LED illumination pattern in detection of malaria parasite in the red blood cells [5]. M. R. Kellman, et al. also proposed a new approach

to optimizing coded-illumination patterns of the LED array microscope for a phase reconstruction algorithm [6]. Among all the microscopy physical parameters, manipulating the optic mask or filter in the lens is not an arduous or impracticable technique. Several filters and optic masks have been studied and commercialized for a long time [7]. For instance, the color filters and other kinds of absorption masks are used to fine-tune the color balance of tungsten and halogen microscope light, or increasing the intensity and saturation of the objects with the specific color. Moreover, several kinds of phase mask such as Double Helix, Single Helix, Tetrapod could modify the point spread function (PSF) to capture 3D information, extend the depth of field, image larger volumes, further help the researchers meet the specific goals. Today, fabricating the customized optic mask or filters would be practicable. In view of this, in this project, I aim to simulate the optics lens of microscope, adding a specially designed optic mask, and then cascading with CNN, to jointly optimize all the parameters by machine learning algorithm. By comparing the performance of different kinds of optics masks setting (i.e. color filter, absorption mask, phase mask) as well as different CNN (i.e. Alexnet, VGG16), this study could assist the researchers to choose the most favorable, and cost-effective physical parameter to manufacture, and make this technique become more feasible and practicable in the real world.

This report is organized as follows: First, the dataset, physical layers, CNN architecture, Train-Test Split and Validation framework would be introduced in Section 2. Next, in Section 3, I would demonstrate the classification results in different physical layer and CNN architectures, as well as final image segmentation performance. Finally, in Section 4, I would discuss the practical consideration of these setting and the future works.

2 Methods

2.1 Dataset [8]

The dataset consists of 5000 histological images, which are RGB 3 channels, 150 x 150 pixels, with resolution equal 0.495 μm per pixel. Each image belongs to exactly one of eight tissue categories: (a) tumour epithelium, (b) simple stroma, (c) complex stroma (stroma that contains single tumour cells and/or single immune cells), (d) immune cell conglomerates, (e) debris and mucus, (f) mucosal glands, (g) adipose tissue, (h) background. As shown in Fig 1.

In addition, there are 10 larger histological images of 5000 x 5000 pixels each. Each of these images contains more than one tissue type. I would use these large figures in the segmentation task to test my model.

2.2 Overall Architecture

Figure 2 shows the overall architecture of this experiment. First, the histology images would pass the simulated optic aperture with (NA = 0.25 Fmax). Next, the images would pass through specially designed optic mask. Finally, CNN models would be applied to perform classification based on the filtered images. In this experiment, I would simulate four different kinds of optic masks (see Figure 3 and Section 2.3), and two different CNN models (see Section 2.4).

2.3 Physical Layer Simulation

As shown in Figure 3, in this experiment, I consider four different scenarios of optic mask:

- **A RGB color filter mask**: Each R, G, B channel would be filtered by its individual real value absorption mask, with absorption magnitude range from 0 to 1. (Figure 3a)
- **Single absorption mask**: A real value absorption mask would be applied on all channels with absorption magnitude range from 0 to 1. (Figure 3b)
- **A non-constraint phase mask**: A complex-value mask without any constraint (the value can be anywhere on the complex plane) (Figure 3c)
- **A constrainted phase mask** : A complex-value mask with magnitude equal to 1. (Figure 3d)

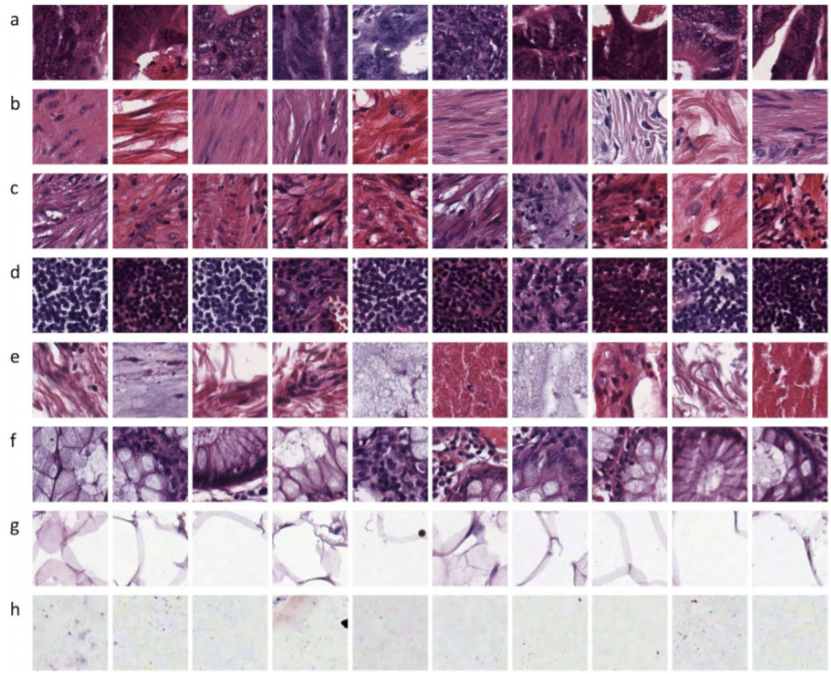

Figure 1: Examples of 8 histology categories

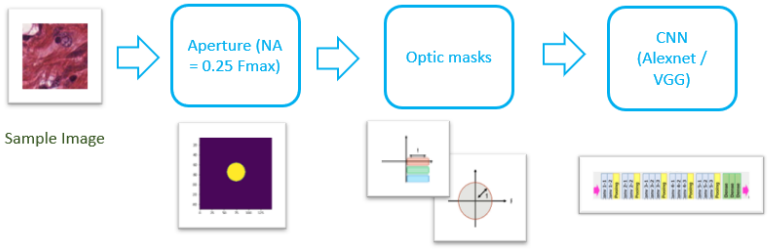

Figure 2: Overall architecture of the experiment

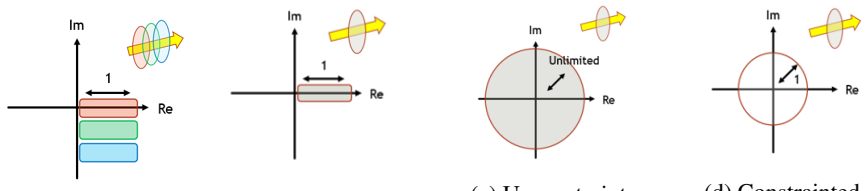

(a) RGB color filter (b) Absorption mask range from 0 - 1 (c) Unconstraint complex mask (d) Constrainted complex mask

Figure 3: Physical Layers design

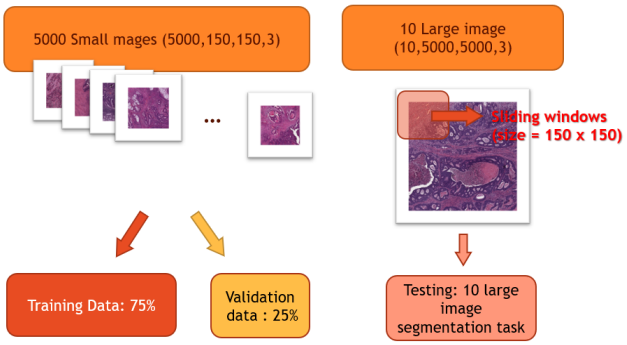

Figure 4: Train-test split and validation

Table 1: Model accuracy of different physical layer and CNN architectures

	Model	RGB filter	Real value absorption mask	Unconstraint Phase mask	constrainted Phase mask
Train	Alexnet	62.74	61.73	**69.78**	64.53
	VGG16	14.72	14.76	16.21	12.88
Validate	Alexnet	66.08	63.27	**69.12**	56.64
	VGG16	15.32	13.44	12.14	11.08

2.4 CNN Architecture

I applied 2 kinds of CNN in this experiment.:

Alexnet [9] : Designed by Alex Krizhevsky et al., Alexnet is a really popular architecture to perform medical diagnosis [10] [11]. It contains 5 convolutional layers intervening few max-pooling layers, follow by 3 fully connected layers.

VGGNet-16 [12]: VGG is a plain and straight forward CNN and is known as its very uniform architecture. The main idea in the VGG is to keep the convolution size small and constant and design a very deep network. VGG is also been used in several medical image classification tasks [13]. In this experiment, I pick VGG16 from VGG family, which consists of 16 convolutional layers.

In order to prevent overfitting, I applied dropout with 40 % rate in the dense layers of both Alexnet and VGG16.

2.5 Train-Test Split and Validation

As shown in Figure 4, I split the 5000 basic images into training and validating sets with 3:1 ratio, and train the model in 10 epoch with batch size = 32. The 10 large images would be used as the final testing set. Using a sliding window with size 150 x 150, I cropped the large image sequentially and conduct the segmentation task, the model would output a segmentation map for each large image.

3 Results

3.1 Performance Evaluation

The classification accuracy of different architectures are listed in Table 1. The best result appears when combining unconstriant phase mask with Alexnet, as shown in bold text in Table 1.

Figure 5 illustrates the curve of training and validation accuracy. We could see that the performance of the validation set is in general comparable with the training set, which might indicate high dropout rate I applied can successfully prevent overfitting. while the validation curve exists a lot of oscillation.

Figure 6 shows the confusion matrix of the best model. First, we can see that the models in general classify each class well. Secondly, there are a lot of encounters in class 6 (adipose tissue) misclassified as class 7 (background), this might not cause a big problem in clinical diagnoses since these tow

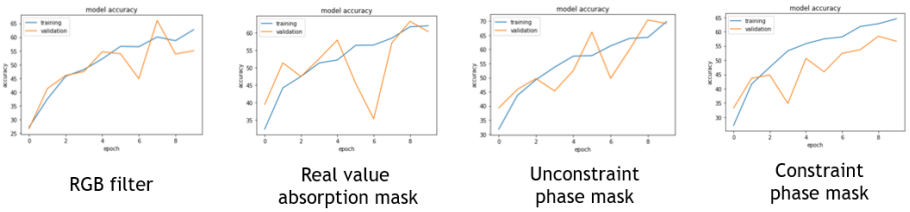

Figure 5: Training and Validation Accuracy v.s. Epoch

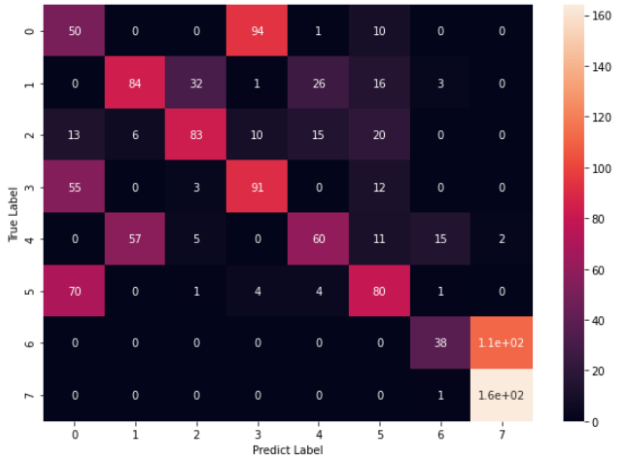

Figure 6: Confusion Matrix

categories are both benign tissues. On the other hand, some encounters in class 0 (tumor epithelium) are misclassified as class 3 (immune cell conglomerates). This false-negative group indicates that some tumor encounter are failed to be identified by CNN, it might be an issue in clinical diagnoses.

3.2 Large Image Segmentation Task

I applied the best Machine Learning architectures: Unconstraint phase mask + Alexnet, to conduct the final image segmentation task. Figure 7 shows the segmentation result of one of the large images. As we can see, the CNN could really discriminate different textures of large samples. It successfully differentiates simple stroma (label 1, purple colormap) with malignant, dark, tumor cells distributed in the upper left part (label 0, green colormap). The intermediate regions would be classified as complex stroma - stroma that contains single tumor cells and/or single immune cells (label 2, yellow colormap). The segmentation result of the remaining large images are shown in Appendix.

4 Discussion

4.1 Comparison of Different Frameworks

In all the physical layer design scenarios, the unconstraint phase mask yield the best performance (70% in validation accuracy), as we expect. However, in the practical scenario, it is nearly impossible to design an unconstriant phase mask. On the other hand, a simple RGB color filter is easier to fabricate, and it also shows a pretty good result (66% in validation accuracy), which might be an ideal and cost-effective physical layer setup to improve the classification accuracy.

Compare two CNN models, VGG16 is cannot be trained successfully. It might because that VGG16 is much more complicated than Alexnet (16 layers v.s. 8 layers, 138M parameters v.s. 61M parameters). In addition, VGG16 initially was trained in a larger dataset which contain hundreds of thousands images, while I only get 5000 training data, hence, I think VGG does not perform ideally in this small dataset (5000 encounters). It is also interesting that another classmate present in April 24 also have a

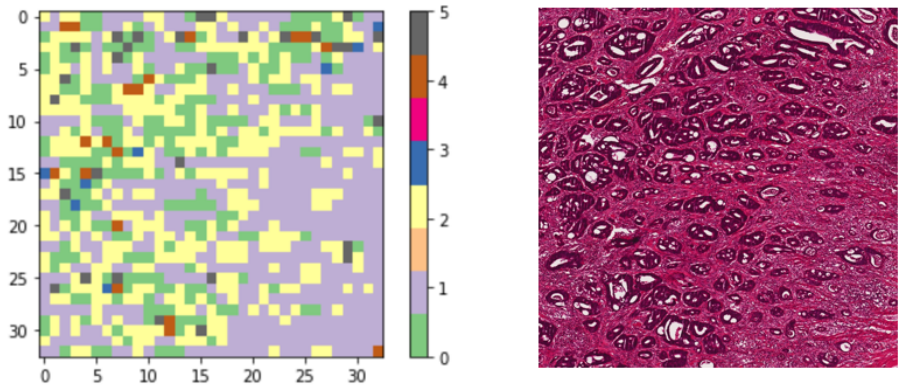

Figure 7: Segmentation result of large image # 1

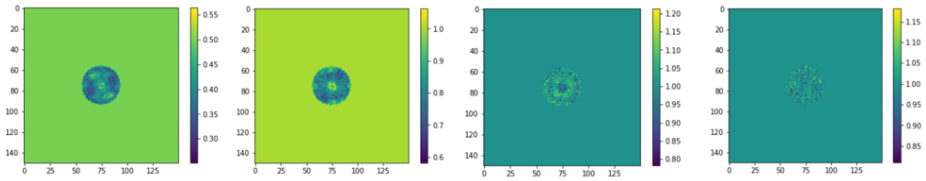

Figure 8: Optic mask visualization. Left: The magnitude of real-value mask (initialize as 0.5, since I constraint it range from 0 to 1). Middle Left: The magnitude of unconstraint phase mask (initialize as 1). Middle Right: The phase angle of unconstraint phase mask (initialize as 1). Right: The phase angle of the constraint phase mask (initialize as 1).

bad result when using VGG16. The application and the limitation of VGG16 in medical image might be worth to be discussed in the future.

4.2 Investigation of the Weight Value

Further we investigate the weight value of different kinds of optic mask.

1. In RGB color filter, the weight value of R,G,B is 0.40: 0.12: 0.51 respectively, approximately in 4:1:5 ratio. Nulling the Green channel might be beneficial to classification of histology.

2. For the Real value mask, there exist a circular ring in the most center part of the mask, as shown in Figure 8 Left. Moreover, there exist a Chinese Tai Chi-like shape in the phase mask. Two Tai-Chi pattern would become darker when training in more epochs, which is really interesting.

3. The magnitude of unconstraint phase mask (Figure 8 Middle Left) is really similar with the weight magnitude of real value mask. As for the phase (angle / rad) of unconstraint phase mask (Figure 8 Middle Right), we got a symmetrical circular patterns.

4. Finally, the phase value (angle/ rad) of the constraint-1 phase mask (Figure 8 Right). The phase pattern remains random-like after training, while the angle would not vary too much.

4.3 Conclusion and Future Work

In this experiment, I systematically examine the performance of different optimized physical layers and CNN frameworks. The results are further verified by an external large histological image segmentation task. Our result could aid the researchers or medical institutions develop more robust Computer Aid Diagnoses tools, satisfying the unmet need in medical field.

In the clinical situation, misclassifying the tumor category as a benign category would be much more serious than misclassifying the benign category A to benign category B. In the future, we can improve the model by change the penalty or cost function of the algorithm, to let the model be useful in the clinical diagnosis situation. In addition, the hyperparameters of CNN models used in this

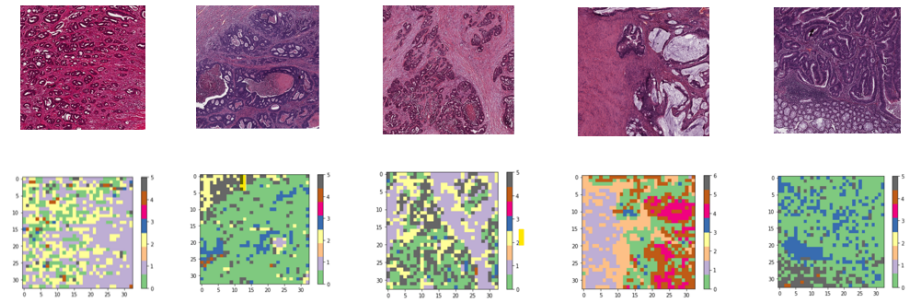

Figure 9: Segmentation result 1 - 5

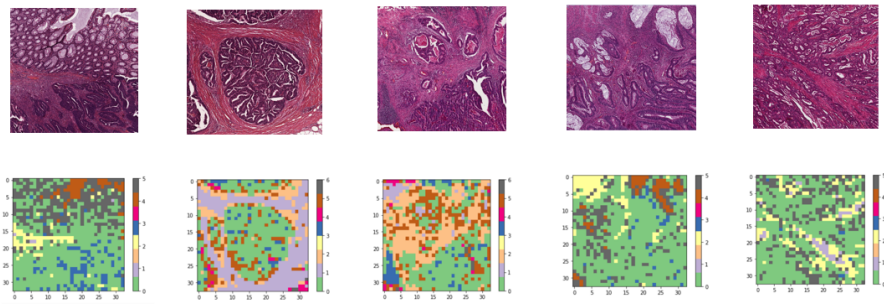

Figure 10: Segmentation result 6 - 10

experiment are all the default setting of the original Alexnet and VGG16, it is possible to change the hyperparameters, customize the model for this task. Or even use the idea of transfer learning: pre-training the models first, and fine-tune using my data, to achieve the better results.

5 Acknowledgments

This work was supported by Duke University BME590L Machine Learning in Imaging Spring 2020 semester.

6 Appendix

- Figure 9, 10: Completed large image segmentation results.
  Labels: (0) tumour epithelium, (1) simple stroma, (2) complex stroma (stroma that contains single tumour cells and/or single immune cells), (3) immune cell conglomerates, (4) debris and mucus, (5) mucosal glands, (6) adipose tissue, (7) background.

References

[1] M. Shapcott, K. J. Hewitt, and N. Rajpoot, "Deep learning with sampling in colon cancer histology," *Frontiers in Bioengineering and Biotechnology*, vol. 7, p. 52, 2019. [Online]. Available: https://www.frontiersin.org/article/10.3389/fbioe.2019.00052

[2] J. Malik, S. Kiranyaz, and S. Kunhoth, "Colorectal cancer diagnosis from histology images: A comparative study." [Online]. Available: https://arxiv.org/ftp/arxiv/papers/1903/1903.11210.pdf

[3] A. Janowczyk1 and A. Madabhushi1, "Deep learning for digital pathology image analysis: A comprehensive tutorial with selected use cases." [Online]. Available: https://www-ncbi-nlm-nih-gov.proxy.lib.duke.edu/pmc/articles/PMC4977982/

[4] R. Horstmeyer, "Convolutional neural networks that teach microscopes how to image." [Online]. Available: https://arxiv.org/pdf/1709.07223.pdf

[5] A. Muthumbi and A. Chaware, "Learned sensing: jointly optimized microscope hardware for accurate image classification." [Online]. Available: https://www.osapublishing.org/boe/abstract.cfm?uri=boe-10-12-6351

[6] M. R. Kellman, E. Bostan, N. Repina, and L. Waller, "Physics-based learned design: Optimized coded-illumination for quantitative phase imaging." [Online]. Available: https://arxiv.org/pdf/1808.03571.pdf

[7] "Double helix optics." [Online]. Available: http://www.doublehelixoptics.com/solutions/

[8] J. N. Kather and C.-A. Weis, "Multi-class texture analysis in colorectal cancer histology." [Online]. Available: https://www.nature.com/articles/srep27988

[9] A. Krizhevsky, "Imagenet classification with deep convolutional neural networks." [Online]. Available: https://papers.nips.cc/paper/4824-imagenet-classification-with-deep-convolutional-neural-networks.pdf

[10] A.Fourcadea and R.H.Khonsarib, "Deep learning in medical image analysis: A third eye for doctors." [Online]. Available: https://www.sciencedirect.com/science/article/pii/S2468785519301582

[11] A. Pedraza and J. Gallego, "Glomerulus classification with convolutional neural networks." [Online]. Available: https://www.researchgate.net/publication/318168077_Glomerulus_Classification_with_Convolutional_Neural_Networks

[12] K. Simonyan and A. Zisserman, "Very deep convolutional networks for large-scale image recognition." [Online]. Available: https://arxiv.org/abs/1409.1556

[13] M. H. Hesamian and X. H. . P. K. Wenjing Jia, "Deep learning techniques for medical image segmentation: Achievements and challenges." [Online]. Available: https://link.springer.com/article/10.1007/s10278-019-00227-x